*** Supporting Information**

Biomineralization of a titanium-modified hydroxyapatite semiconductor on conductive wool fibers.

Alessio Adamiano [a] *, Nicola Sangiorgi [a], Simone Sprio [a], Andrea Ruffini [a], Monica Sandri [a], Alessandra Sanson [a], Pierre Gras [b,f], David Grossin [b], Christine Francès[f], Konstantinos Chatzipanagis [c], Matthew Bilton [c], Bartosz Marzec [d], Alessio Varesano[e], Fiona Meldrum [d], Roland Kröger [c] and Anna Tampieri [a]

[a] *Institute of Science and Technology for Ceramics (ISTEC), National Research Council (CNR), Via Granarolo 64, 48018 Faenza, Italy*

[b] *CIRIMAT, Université de Toulouse,, CNRS/INPT/UPS UMR 5085, Ensiacet, 4 allée Emile Monso, 31030 Toulouse Cedex 4, France.*

[c] *Department of Physics, University of York, York YO10 5DD, U.K.*

[d] *School of Chemistry, University of Leeds, Woodhouse Lane, Leeds LS2 9JT, U.K.*

[e] *CNR-ISMAC, Institute for Macromolecular Studies, C.so G. Pella 16, 13900 Biella, Italy*

[f] *Laboratoire de Génie Chimique, Université de Toulouse, CNRS/INPT/UPS UMR 5503, Ensiacet, 4 allée Emile Monso, 31432 Toulouse Cedex 4, France.*

*Author for correspondence: Dr. Alessio Adamiano

Institute of Science and Technology for Ceramics (ISTEC)
National Research Council (CNR),
Via Granarolo 64, 48018 Faenza (RA), Italy.
E-mail: alessio.adamiano@istec.cnr.it
Tel: +39 0546699761

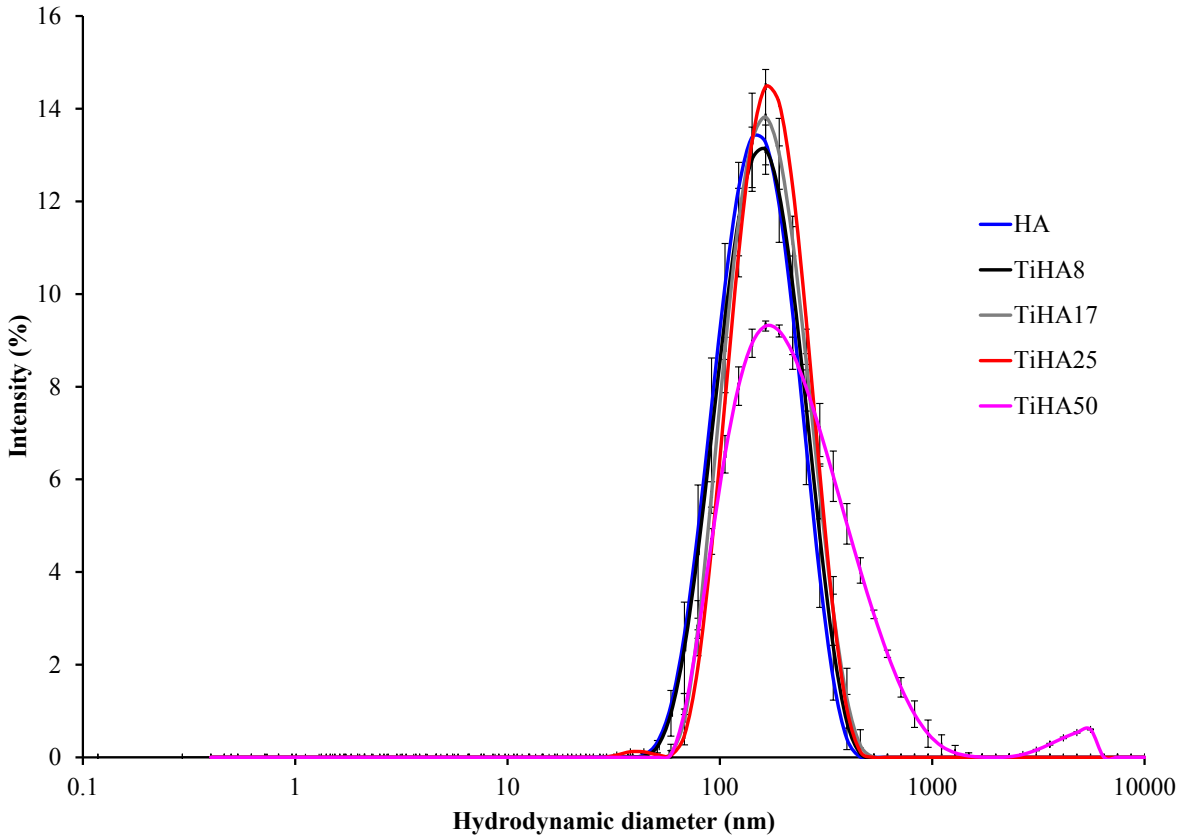

Figure S1. Hydrodynamic diameter size distribution expressed as average intensity of scattered light from n = 10 DLS measurements for each sample. The error bars represent the relative standard deviation for each data point.

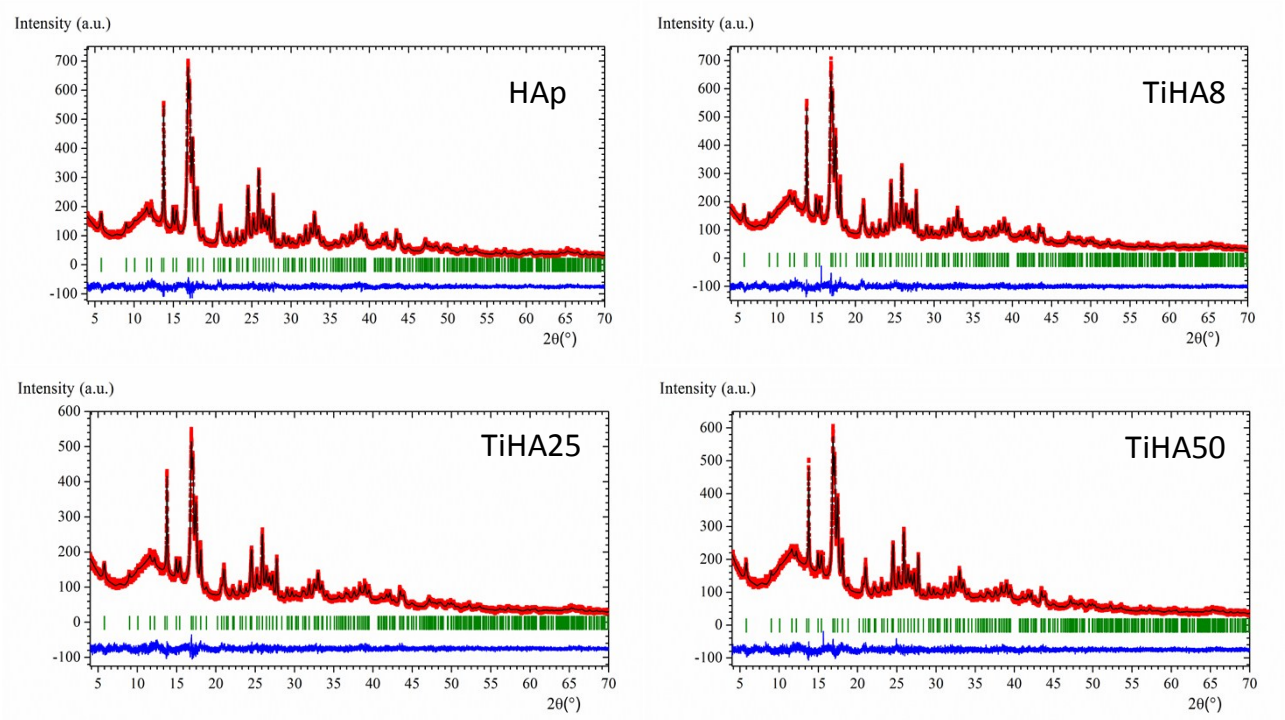

Figure S2. HR-PXRD patterns of HAp, TiHA8, TiHA25 and TiHA 50. Observed data points are indicated by red dots and the simulated diagrams by the black line. The difference between them is indicated by the blue line; vertical green lines indicates the Bragg peak positions.

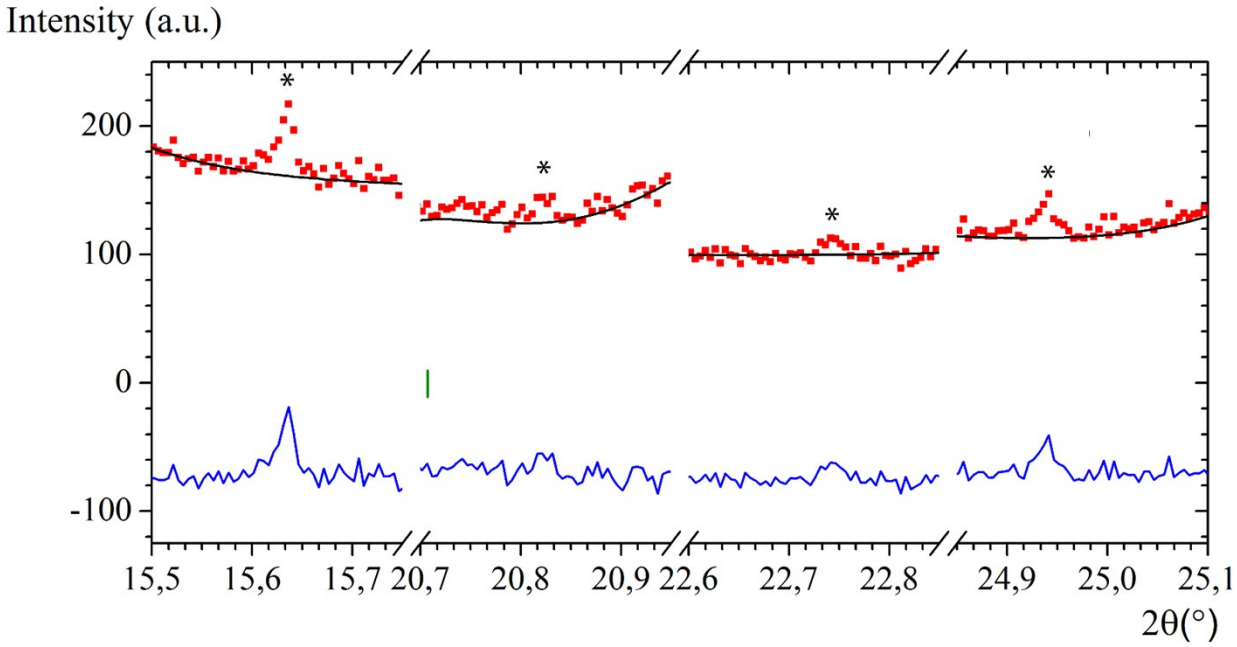

Figure S3. Representation of the 4 diffraction peaks ascribable to the presence of a third phase beside the apatitic and the amorphous one, tentatively identified as calcium titanium phosphate ($CaTi_4(PO_4)_6$) in the HR-PXRD pattern of TiHA50 collected using synchrotron radiation. Observed data points are indicated by red dots and the simulated diagrams by the black line. The difference between them is indicated by the blue line.

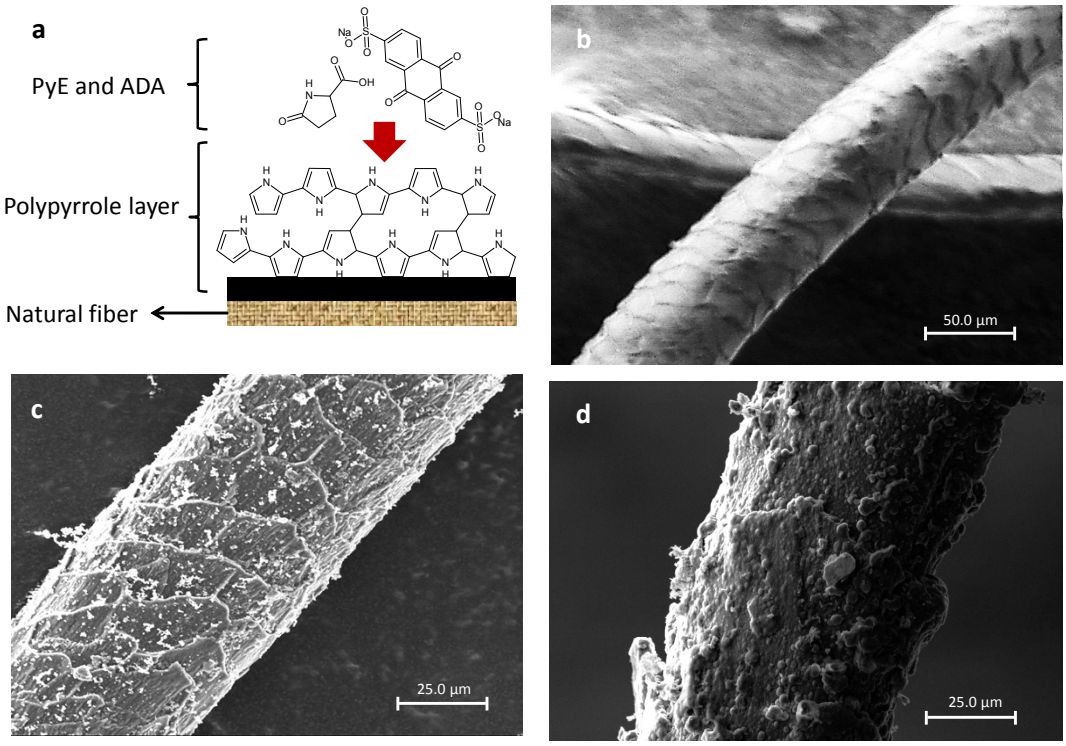

Figure S4. Schematized cross-section view of the PPy-coated conductive wool fiber showing the molecular structures of the PPy layer, pyroglutamic acid and antaquinon-2-sulfonic acid (a) with SEM pictures of bare wool fibers (b), wool fibers coated with ADA-doped PPy (WAP) (c) and wool fibers coated with ADA and PyE doped PPy (WAEP5) (d).

Table S1. Zeta potential in HEPES buffer (pH 7.4) and Zeta average in citrate buffer (pH 6.0) of TiHAs determined by DLS analysis.

	Zeta Potential (mV)	Z-average size(nm)	Pdi
HAp	-7.29 ± 0.55	136.27 ± 0.25	0.14 ± 0.02
TiHA8	-14.53 ± 0.23	134.97 ± 0.45	0.14 ± 0.01
TiHA17	-18.23 ± 1.71	154.03 ± 0.93	0.12 ± 0.01
TiHA25	-12.57 ± 0.32	153.43 ± 0.83	0.10 ± 0.01
TiHA50	-14.67 ± 0.51	189.77 ± 1.66	0.25 ± 0.00

Table S2 The microstructural analysis, microstrain and crystallite size, of the TiHA samples.

	Orientation	Size (nm)	Strain (%)
HAp	(001)	60.1 (29)	15(6)
	-(100)/(010)	24.4(4)	10(5)
	(110)-	22.3(3)	10(5)
TiHA8	(001)	66.9(37)	17(5)
	-(100)/(010)	26.8(5)	8(4)
	(110)-	24.9(4)	8(4)
TiHA25	(001)	59.7(38)	18(6)
	-(100)/(010)	24.4(5)	11(5)
	(110)-	22.7(4)	11(5)
TiHA50%	(001)	67.8(45)	16(7)
	-(100)/(010)	28.2(6)	9(3)
	(110)-	25.3(5)	9(3)

Table S3. Weight percent of PPy on wool fibers, and electric resistance of PPy-coated wool fibers doped with ADA at increasing concentration of PyE. Average resistance values and standard deviation from eight tests are reported.

Sample	ADA mol%	PyE mol %	PPy wt%	Resistance kΩ/cm
WAP	25	-	13	4.73 ± 3.04
WEAP5	25	5.0	17	1.12 ± 0.31
WEAP10	25	10.0	19	1.84 ± 0.50